ACGT 2012, Asian Congress on Gas Turbines 2012,
August 20-22, 2012, Shanghai, P.R.China

ACGT2012-1084

Simulation of a Gas Turbine Cascade within the Full Test Cell Environment

R O Evans[1], Q Zhang[2], W Chen[2], W N Dawes[3] & C F Favaretto[4],
[1]Cambridge Flow Solutions Ltd, Compass House, Vision Park, Cambridge UK,
[2]University of Michigan-Shanghai Jiao Tong University Joint Institute,
Shanghai Jiao Tong University, Shanghai, China,
[3]Cambridge University Engineering Department, Cambridge UK
[4]BoXeR Solutions KK, Kobe, Japan

ABSTRACT

This paper describes the simulation of a cascade of transonic turbine blades within the full test cell environment. The objective of this simulation is to understand various installation issues which go into the design of the test cell. The focus here is on creating periodic test conditions in a cascade with relatively few blades and transonic exit. Using a Design of Experiment methodology a series of simulations was performed with a systematic variation in both suction and pressure side tailboard locations. The flow relative to the target test blade was optimized with respect to a reference periodic condition.

INTRODUCTION

Testing of gas turbine blades within a specialized, well-understood test cell environment remains a key part of the overall design process. For reliable, useful data a range of scales need to be managed and the full complexity of the geometry confronted.

At the *micro*-scale are the blades themselves, typically installed in a cascade with some sort of tail-board and associated instrumentation. At the *meso*-scale is the integration of the blade cascade within a test chamber with the associated risks of distorted boundary conditions. At the *macro*-scale is the overall performance of the test cell: inlet flow smoothness to the test chamber, start-up transients, balancing Mach number & Reynolds number against pressure level and power consumption. The design and commissioning of a successful test environment represents a significant engineering challenge.

In this paper we show the first-of-a-kind simulation of a full test cell environment showing how the power of CFD can be brought to bear on this challenge. In particular, the positioning of the suction and pressure side tailboards is optimized with respect to the periodicity of the test blade.

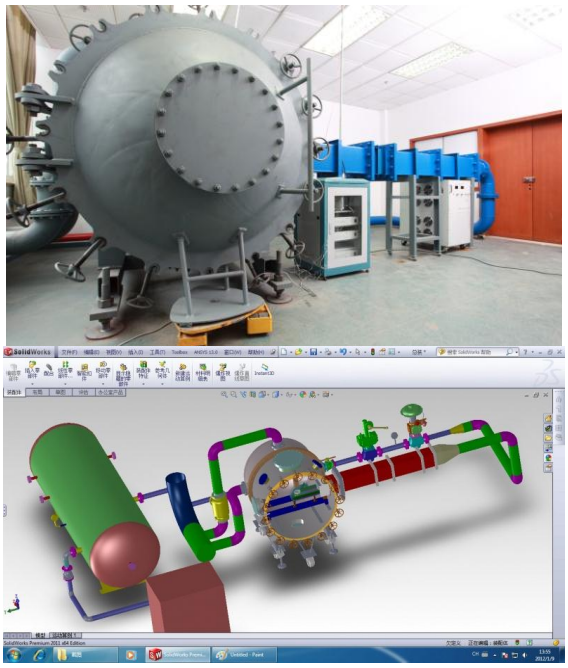

Fig.1: Overview and CAD model of the UM-SJTU cascade tunnel (we are grateful to the Shanghai Jiao Tong University/University of Michigan Joint Institute for permission to use this geometry)

SETTING UP THE SIMULATION

Geometry & Meshing

The key bottleneck in attempting such an ambitious simulation is generating a mesh for the extensive and very complex geometry; an overview

and CAD model of the rig is shown in Figure 1. Over recent years a series of papers (Dawes *et al* [2005-2011]) have described a step-change in mesh generating capability based on the radically different approach to both geometry and mesh generation which has grown up to support physics-based animation in the film and computer games industry – see for example Baerentzen [2001] and Galyean *et al* [1991] and the annual SIGGRAPH Conference series. The key to this is to regard the geometry as *implicit*, represented by a distance field, captured on an octree and managed as a Level Set (see Adalsteinsson *et al* [1995] for example). This allows great freedom as the geometry can then be handled as a scalar variable, can support a variety of Boolean operations (allowing geometry to be "added" or "subtracted" for example) – and parallelised trivially. The main disadvantage is that the geometry is not quantitative in the sense that in animation if the wizard looks like a wizard then it is a wizard! For scientific/engineering simulation the geometry *must* be faithfully represented. The resulting meshing system, *BoXeR*, is an automatable system capable of dealing with *true* geometry and overcoming all the disadvantages of the conventional approaches to mesh generation (see for example Shontz [2010]).

The *BoXeR* meshing system consists of five stages – each of which required substantial technical innovation:

1. The first stage captures the geometry digitally (like a 3D photograph) via a dynamically load balanced bottom-up octree based on very efficient space filling curve technology (the traditional top-down octree is difficult to implement in parallel); this background mesh supports the imported geometry as a solid model using distance fields managed as a Level Sets
2. Next, a conjugate body-conformal hybrid mesh is constructed using shape insertion, to allow the octree to better match the body curvature, followed by snapping to the actual surface; the key technology here is mesh smoothing driven by a series of mesh quality metrics (skew, warpage, cell-to-cell variation, etc.)
3. Viscous layer meshes are then inserted using the distance field as a guide – formally the gradient of the distance field is the surface normal and so issues like geometry corners or geometry proximity are much easier to manage
4. Active feature detection for sharp corners and for thin/zero thickness geometries is required as the geometry is held implicitly; this make use of local mesh topology swapping and smoothing
5. Finally ALL of the algorithms are implemented in parallel - including most of the i/o using HDF5 – so that scalability to huge problem sizes is straightforward and automatic.

The following Figures illustrate these stages (much more detail is provided in Dawes *et al* [2005-2011).

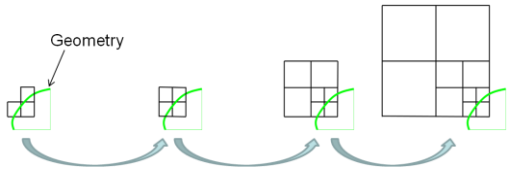

Fig.2: Bottom-up octree meshing (from Dawes *et al* [2010])

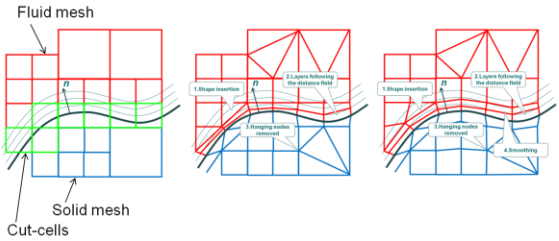

Fig.3: Body-fitted hybrid mesh construction (from Dawes *et al* [2010])

Application to the UM-SJTU turbine test rig shown earlier in Figure 1 is a routine meshing task: *BoXeR* meshed this entire rig with ~50M cells by importing direct the manufacturing CAD with no need for cleaning or de-featuring in a wall-clock time of about half an hour. A wide range of scales is resolved – the blade is resolved down to Y+~10 – the details of the honeycomb flow straighteners are similarly well resolved.

Flow Solution

The subsequent flow simulation was performed with CFX™ using standard code settings. Some aspects of the results are shown in Figure 4-6. Figure 4, shows a *macro* view, Figure 5 a *meso* view and Figure 6 a *micro*-view. The flow scales captured range from the detail of the blade surface pressure distribution to the highly swirling and distorted flow in the settling chamber and cascade tank. In Figure 6 the mesh is coloured with static pressure from the simulation and as can be seen with the current, arbitrary tailboard setting the cascade is not fully periodic.

A significant advantage of being able to perform an integrated CFD simulation is that the tailboards can be quickly adjusted to maximize periodicity. A rapid series of simulations could then be performed to help design the rig and manage its operation. For example, Figure 7 shows shock structures, visualized via the density field, at two different tail-board positions (the second essentially open jet). This suggests that it would be both very useful and feasible to perform a systematic study of cascade

periodicity, set up as a classical optimization problem, or Design of Experiment.

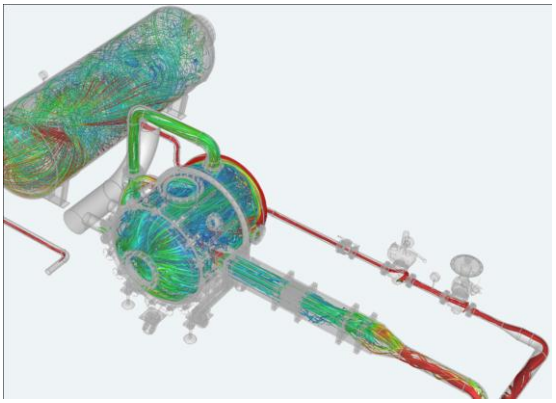

Fig.4: Macro-scale: overview of simulation

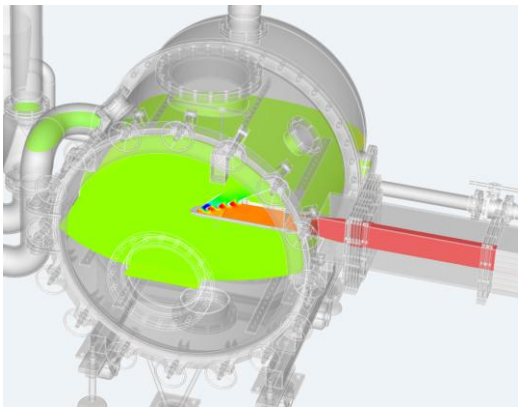

Fig.5: Meso-scale view of the simulation

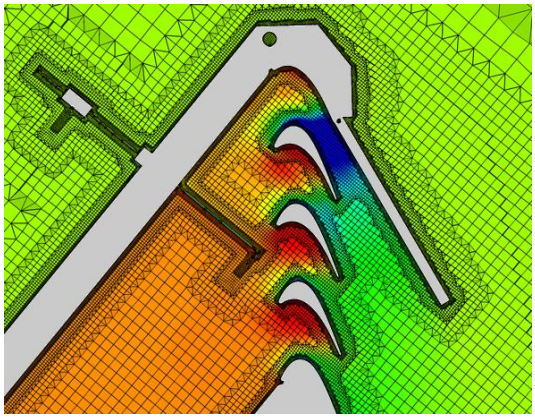

Fig.6: Micro-scale view of the simulation (these particular blades are taken from Thorpe et al [2004])

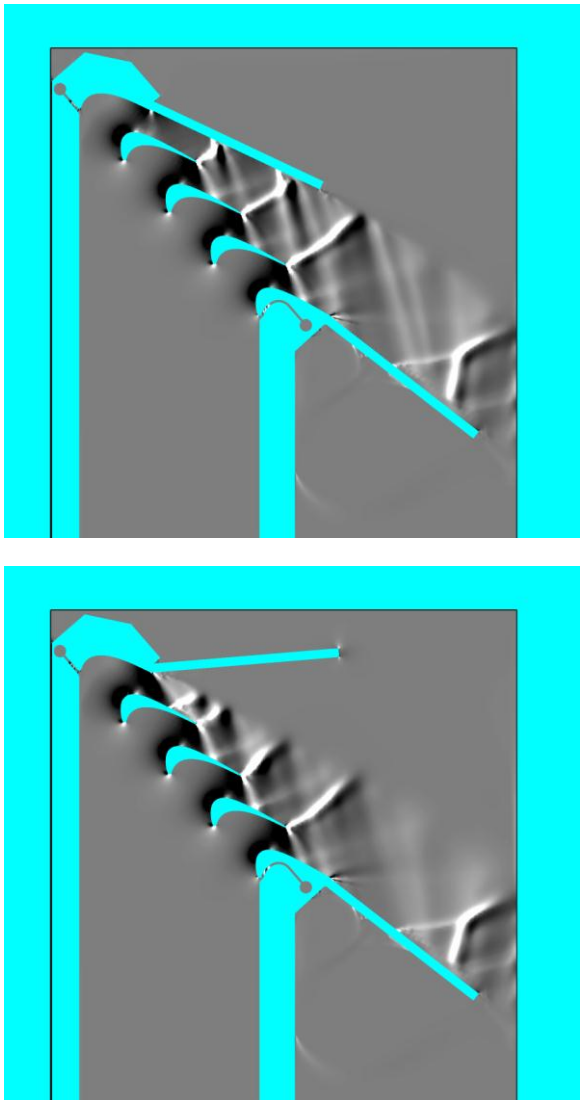

Fig.7: Shock structures, visualized via the density field, at two different tail-board positions (the second essentially open jet)

OPTIMISATION via DESIGN of EXPERIMENT

The classical Design of Experiment, "DoE", proceeds by making a systematic choice of a range of design parameters, performing a flow simulation for each combination of parameters and then fitting a low order model (for example a Response Surface) to the resulting variation in objective function. This can then be used to choose the optimum set of design parameters. This section describes the various building blocks which make up this approach.

The first is the objective function to be optimized. Here we are focused on periodicity and so define a *reference* blade pressure distribution obtained from a truly periodic flow simulation, see Figure 8. The

objective function is computed as the rms difference between this reference and the actual pressure distribution obtained from each individual simulation.

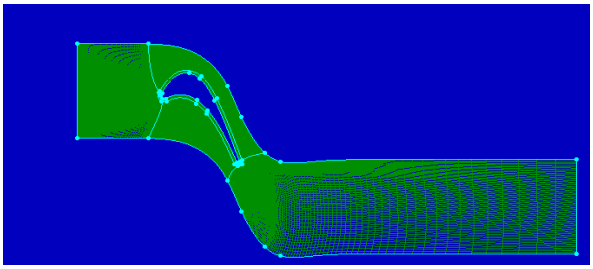

Fig.8: *Reference* periodic blade simulated in FLUENT™ with a multi-block structured mesh

Next is the *parameterisation* which for this study consisted of variable locations for the suction and pressure side tailboards. Figure 9 shows the computational domain and range of movement for the tailboards. There were 8 pressure side positions and 7 suction side positions in the DoE leading to 56 cases run.

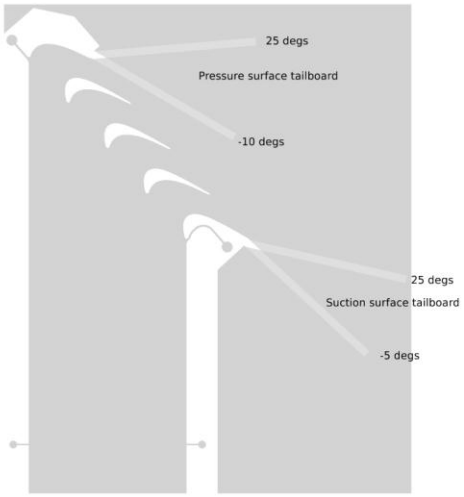

Fig.9: Computational domain and range of movement for tailboards; the DoE consisted of 8 PS positions x 7 SS positions = 56 cases run

The DoE is then implemented as an *integrated workflow* to permit full automation. One of the key advantages of the *BoXeR* meshing system is that it can easily be scripted within such a workflow and will continue to deliver high quality, solvable meshes with very high robustness over a very wide range of parameterized geometries. Figure 10 shows the DoE flowchart – scripted using Python and executed completely automatically. The results will be presented and discussed in the next section.

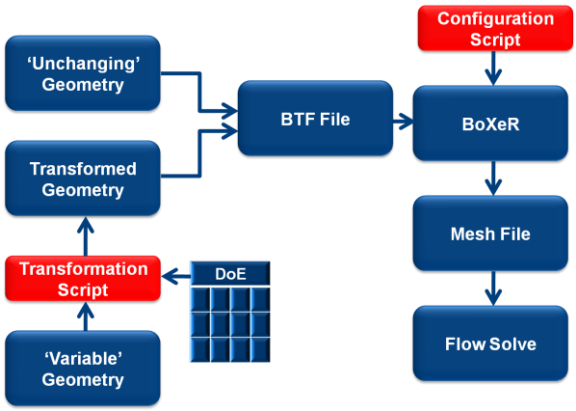

Fig.10: DoE flowchart

RESULTS

The objective of the DoE is to find tailboard locations which will allow the test blade to operate most closely to that in a periodic flow. Figure 11 shows blade surface isentropic Mach number distribution for all 56 cases – compared to the reference distribution shown in red. The pressure side of the blade is rather insensitive to tailboard location but there is very significant variability on the suction side – as would be expected for this transonic operating point.

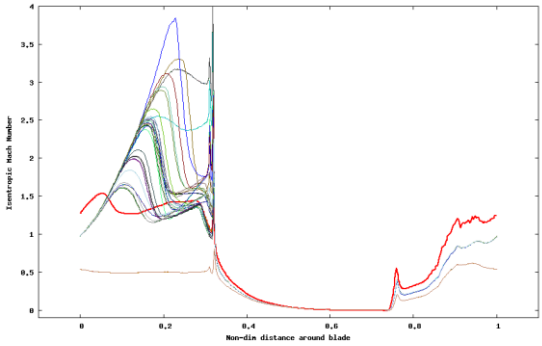

Fig.11: Blade surface isentropic Mach number distributions during the DoE with the target, fully periodic distribution shown in red.

The final step was to fit a low order model, a piecewise linear Response Surface, to the data. Each result is represented via the objective function computed as the rms difference between the reference and the actual pressure distribution obtained from each individual simulation. This is plotted in Figure 12. The position of the pressure side tailboard has the largest affect on the change in isentropic Mach number distribution. There is a clear optimal 'trough' at a pressure side tailboard angle of -5 degrees and the corresponding position for the suction side

tailboard seems to be -5 degrees. Overall, although not quite perfect, this optimum enables a satisfactory periodic flow for the test blade.

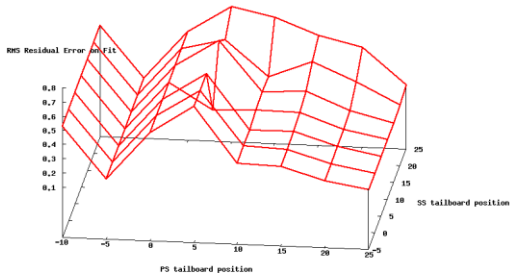

Fig.12: Response Surface fitted to the DoE showing RMS error plotted versus PS and SS tailboard positions

CONCLUSIONS

This paper has shown how the power of CFD can be brought to bear on the complex problem of designing and managing a large, sophisticated test rig. In particular the effect of potential distortion of the flowfield relative to the cascade of blades under test can be studied.

The study here was concerned with the effect of tailboard location on cascade periodicity and an optimum location was identified.

In future work we plan to study the design of the tailboards themselves by parametrically introducing porosity – perhaps via variable slots.

ACKNOWLEDGEMENTS

We are grateful to the Shanghai Jiao Tong University/University of Michigan Joint Institute for permission to use this geometry.

REFERENCES

Adalsteinsson D & Sethian JA "A level set approach to a unified model for etching, deposition & lithography II: three dimensional simulations" J.Comput.Phys, 122, 348-366, 1995

Baerentzen A "Volume sculpting: intuitive, interactive 3D shape modelling" IMM, May 2001

Dawes WN "Building Blocks Towards VR-Based Flow Sculpting" " 43rd AIAA Aerospace Sciences Meeting & Exhibit, 10-13 January 2005, Reno, NV, AIAA-2005-1156

Dawes WN, Kellar WP, Harvey SA "Towards a fully integrated parallel geometry kernel, mesh generator, flow solver & post-processor" 44th AIAA Aerospace Sciences Meeting & Exhibit, 9-12 January 2006, Reno, NV, AIAA-2006-45023

Dawes WN, Kellar WP, Harvey SA "Viscous Layer Meshes from Level Sets on Cartesian Meshes" 45th AIAA Aerospace Sciences Meeting & Exhibit, 8-11 January 2007, Reno, NV, AIAA-2007-0555

Dawes WN, Kellar WP, Harvey SA "Towards topology-free optimisation: an application to turbine internal cooling geometries" 46th AIAA Aerospace Sciences Meeting & Exhibit, 7-10 January 2008, Reno, NV, AIAA-2008-925

Dawes WN, Kellar WP, Harvey SA "A practical demonstration of scalable parallel mesh generation" 47th AIAA Aerospace Sciences Meeting & Exhibit, 9-12 January 2009, Orlando, FL, AIAA-2009-0981

Dawes WN, Kellar WP, Harvey SA "Generation of conjugate meshes for complex geometries for coupled multi-physics simulations" 87th AIAA Aerospace Sciences Meeting & Exhibit, 7-10 January 2010, Orlando, FL, AIAA-2010-062

Galyean TA & Hughes JF "Sculpting: an interactive volumetric modelling technique" ACM Trans., Computer Graphics, vol.25, no.4, pp 267-274, 1991

Shontz S, Editor, Proceedings of the 19th International Meshing Roundtable, Chattanooga TN, 2010

Thorpe S.J., Yoshino ,S., Ainsworth R.W., and Harvey N.W., "An investigation of the heat transfer and static pressure on the over-tip casing wall of an axial turbine operating at engine representative flow conditions. (I). Time-mean results." International Journal of Heat and Fluid Flow 25 (2004) 933–944

-oOo-